# CircStrn3 Targeting microRNA-9-5p Is Involved in the Regulation of Cartilage Degeneration and Subchondral Bone Remodeling in Osteoarthritis

**Bin Li**
Shanghai Jiao Tong University Medical School Affiliated Ruijin Hospital
**Tao Ding**
Shanghai Jiao Tong University Medical School Affiliated Ruijin Hospital
**Haoyi Chen**
Shanghai Jiao Tong University Medical School Affiliated Ruijin Hospital
**Changwei Li**
Shanghai Jiao Tong University Medical School Affiliated Ruijin Hospital
**Bo Chen**
Shanghai Jiao Tong University Medical School Affiliated Ruijin Hospital
**Xing Xu**
Shanghai Jiao Tong University Medical School Affiliated Ruijin Hospital
**Ping Huang**
Shanghai Jiao Tong University Medical School Affiliated Ruijin Hospital
**Fangqiong Hu**
Shanghai Jiao Tong University Medical School Affiliated Ruijin Hospital
**Lei Guo** ( guolei_sjt@126.com )
Shanghai Jiao Tong University Medical School Affiliated Ruijin Hospital

**Research article**

**Keywords:** Osteoarthritis, CircStrn3, microRNA-9-5p, kruppel-like factor 5, exosomes

**Posted Date:** November 8th, 2021

**DOI:** https://doi.org/10.21203/rs.3.rs-1037235/v1

# Abstract

**Background:** Osteoarthritis (OA) is the most frequent chronic degenerative joint disease, which is a “whole joint” disease including the pathological changes in the cartilage, subchondral bone and the synovium. Mechanical instability is the initiation of the development of OA.

**Methods:** Minus RNA sequencing, fluorescence in situ hybridization and quantitative real-time PCR were used to detect the expression of circStrn3 in human and mouse OA cartilage tissues and chondrocytes. Stimulate chondrocytes to secrete exosomes miR-9-5p by stretching strain. Intra-articular injection of exosomes miR-9-5p into the OA model induced by the operation of instability of the medial meniscus in mice.

**Results:** In the present study, minus RNA sequencing data showed that tensile strain could decrease the expression of circStrn3 in chondrocytes. The results of fluorescence in situ hybridization and quantitative Real-time PCR showed that circStrn3 expression was significantly decreased in human and mouse OA cartilage tissues and chondrocytes. CircStrn3 could inhibit matrix metabolism of chondrocytes through competitively 'sponging' miRNA-9-5p targeting kruppel-like factor 5 (KLF5), indicating that the decreasing of circStrn3 might be a protective factor in mechanical instability-induced OA. Further studies showed that the tensile strain stimulated chondrocytes to secrete exosomes miR-9-5p. Exosomes with high miR-9-5p expression from chondrocytes could inhibit osteoblasts differentiation by targeting KLF5. In addition, intra-articular injection of exosomal miR-9-5p obviously alleviated the progression of OA induced by destabilized medial meniscus surgery in mice.

**Conclusions:** Taken together, these results demonstrated that the reduction of circStrn3 caused the increasing of miR-9-5p, which acted as a protective factor in mechanical instability-induced OA and provided a novel mechanism of communication among joint components and a potential application for the treatment of OA.


# 1. Background

Osteoarthritis (OA) is the most common degenerative joint disease, afflicting mainly the weight-bearing joints, like hips and knees, and is the leading cause of physical disability in elderly population.[1] Currently, the effective treatment to stop the development of OA is limited due to the lack of mechanistic understanding of OA. Injuries directly leading to joint instability are highly associated with OA, suggesting that mechanical instability is a critical factor for the development of OA.[2] However, the exact mechanisms of OA as a result of injury-induced mechanical changes have not been fully elucidated.

Dysfunction of articular chondrocytes and breakdown of cartilage extracellular matrix (ECM) caused by abnormal mechanical stimulations have gained widespread acceptance as the leading causes of articular cartilage degradation.[3] Recently, the pathological changes of the entire joint, including the degenerated cartilage and sclerosis subchondral bone, are the impetus for generally recognizing OA as a disease of the joint as an organ. Mounting evidences suggested that cartilage degeneration and

subchondral bone sclerosis not only were independent drivers of pain, poor function and structural progression of OA, but also influenced each other through pro-inflammatory mediators, growth factors, cytokines and direct cell interacts.[4] Thus, exploring the underlying mechanisms by which chondrocytes under abnormal mechanical stimulations indirectly affect subchondral bone contribute to uncover the pathogenesis of OA.

Circular RNAs (circRNAs), a novel class of endogenous noncoding RNAs,[5] can regulate gene expression at the transcriptional or post-transcriptional level through competitively 'sponging' microRNAs (miRNAs). MiRNAs play an important regulatory role in cell differentiation, apoptosis, and cancer.[6] MiRNAs regulate gene expression through the inhibitory engagement of complimentary “seed sequences” within the 3'-untranslational region (3'-UTR) of target mRNAs, leading to translational inhibition and/or mRNA degradation.[7] The circRNAs-miRNAs-mRNA participate in articular cartilage degradation caused by inflammatory factors or oxidative stress. MiRNAs-enriched exosomes mediate cell-to-cell communications and modulate many biological processes.[8,9] However, whether circRNAs-miRNAs-mRNA participate in the pathogenesis of joint instability-induced OA needs to be further explored.

In this study, minus RNA sequencing data showed that tensile strain decreased the expression of circStrn3 in chondrocytes. CircStrn3 expression was also significantly downregulated in human and mouse OA cartilage tissues and chondrocytes. Further study revealed that circStrn3 could inhibit matrix metabolism of chondrocytes through competitively 'sponging' miRNA-9-5p targeting kruppel-like factor 5 (KLF5), indicating that the decreasing of circStrn3 might be a protective factor in mechanical instability-induced OA. In addition, the tensile strain stimulated chondrocytes to secrete exosomal miR-9-5p. Exosomes with high miR-9-5p could inhibit osteoblasts differentiation. At last, intra-articular (IA) injection of exosomal miR-9-5p obviously alleviated the progression of OA caused by destabilized medial meniscus (DMM) surgery in mice. Taken together, these results indicated a novel mechanism of communication among joint components and providing a potential application for the treatment of OA.

## 2. Materials And Methods

## 2.1. Human knee cartilage procurement

Normal human knee cartilage (subjects aged 55-88 yr, 50% female) samples were obtained from trauma donor with lower limb amputation. Human OA cartilage was obtained from the knees of patients with a diagnosis of advanced OA (patients aged 55-85 yr, 50% female) who underwent total knee arthroplasty. Non-OA cartilage is defined as cartilage with no histologic evidence of degeneration. OA specimens obtained at the time of surgery were examined by the authors and confirmed to have gross evidence of OA (thinning or localized loss of cartilage and focal eburnation) and the histologic diagnosis of OA. Ethical approval was obtained from the Shanghai Ruijin Hospital review board for human knee cartilage samples. All patients gave informed consent.

## 2.2 Animal experiments and ethics

Adult male C57BL/6 mice were used to induce OA model by DMM surgery (four groups and in each group *n = 6*, eight weeks old), following the transection of the medial meniscotibial ligament as previously described.[10] In sham operation group, mice were performed by opening the joint capsule only. At 1 week after DMM surgery, 5 μL exosomes isolated from miR-9-5p overexpressed chondrocytes were IA injected once a week for next 10 weeks. Injection of exosomes isolated from miR-NC overexpressed chondrocytes was used as control. All animal experiments were performed according to the protocol approved by the Shanghai Jiao Tong University (SJTU) Animal Care and Use Committee.

## 2.3. Radiological evaluation and histological staining analyses

The plain radiographs of the mouse knees were obtained by a MX-20 Cabinet X-ray System (Faxitron, Tucson, AZ, USA) and the SkyScan1172 high-resolution micro-CT (Bruker, Kontich, Belgium) was used to reconstruct knee joints as previously described.[11] Samples were fixed in 4% paraformaldehyde overnight, followed by decalcification in EDTA-buffered saline solution (pH 7·4, 0·25 M) for 21 days. The samples were then cut into 6μm sections longitudinally after dehydrated and embedded in paraffin. Hematoxylin-eosin (HE) staining and safranin Ofast green staining were applied to analyze histological changes and cartilage lesions. Collagen type II α 1 (Col2α1) and matrix metalloproteinase 13 (MMP13) antibodies were incubated for immunohistochemistry.

## 2.4. Chondrocyte culture and tensile strain loading

Chondrocytes were isolated from articular cartilage in the knee joints of mice and human as previous report.[12] Articular cartilage tissues were cut into small pieces (< $1mm^3$) and digested with 0·25% trypsin for 30 minutes, followed by digestion with 0·2% type II collagenase for 4 hours. The released cells were cultured in DMEM/F12 media supplemented with 10% fetal bovine serum (FBS) and antibiotics. Once reached to 80% confluence, the cells were subjected to cyclic tensile strain with a 0·5 Hz sinusoidal curve at 5-20% elongation for 12-48 h using an Flexcell1 FX-5000™ Tension System as described in the manufacturer's manual (Flexcell International Corporation, Burlington, NC). Only cells with less than 2 passages were used in order to preserve chondrocyte phenotype.

## 2.5. RNA fluorescence in situ hybridization (FISH) and immunofluorescence

The cicrStrn3 and miR-9-5p fluorescence in situ hybridization (FISH) staining kit for tissues and cells were purchased from GenePharma (Shanghai, China) and the procedure of the staining was according to the instructions. Immunofluorescence staining was obtained by previous protocol.[13] The cells were incubated with mouse antiCOL2α1 antibody (1:100, Abcam Cat# ab34712, RRID: AB_731688), anti-MMP13 antibody (1:100, Abcam Cat# ab39012, RRID: AB_776416) and anti-Runx2 antibody (1:200, Abcam Cat# ab76956, RRID: AB_1565955), followed by fluorescence-linked secondary antibodies for 1h. FISH and fluorescence results were acquired by the Laser scanning confocal microscopy (LSM800, ZEISS).

## 2.6. Quantification of mRNA and Real-time Quantitative PCR (qRT-PCR) Detecting System

Total RNA from tissues and cells were extracted using Trizol reagent (Takara) and then synthetized into complementary DNA (cDNA) by a RevertAid First Strand cDNA Synthesis Kit (Takara). The qRT-PCR was applied using the SYBR Premix Ex Tag Kit (Takara). The primer sequences used in this study were described in Table 1 and Table 2.

Table 1
Primers for qRT-PCR analysis.

| Gene | Forward Primer | Reverse Primer |
|---|---|---|
| *Col2* | 5'-TACTGGAGTGACTGGTCCTAAG-3' | 5'-AACACCTTTGGGACCATCTTTT-3' |
| *Mmp13* | 5'-CTTCCTGATGATGACGTTCAAG-3' | 5'-GTCACACTTCTCTGGTGTTTTG-3' |
| *Adamts5* | 5'-GGCAAATGTGTGGACAAAACTA-3' | 5'-GAGGTGCAGGGTTATTACAATG-3' |
| *Alp* | 5'-AGATGACTACAGCCAAGGT-3' | 5'-CTCCACGAAGAGGAAGAAG-3' |
| *Runx2* | 5'-TACTATGGCACTTCGTCAGGA-3' | 5'-GATTCATCCATTCTGCCACTA-3' |
| *Osterix* | 5'-CAGGCTATGCTAATGATTACC-3' | 5'-GGCAGACAGTCAGAAGAG-3' |
| *circPdia5* | 5'- GCGGCTCCGTTTATCACCTG -3' | 5'- GTCTGAAGTCATGGGGCGTG -3' |
| *circInpp5f* | 5'- CTGCTGCTGCTGTCTAACGC -3' | 5'- CCTGCTGATGGAGTCACCGT -3' |
| *circAdcy5* | 5'- ATGCCTGTGTGAAGCATCCTG -3' | 5'- AACTTGTCAAAGCGGGCGAA -3' |
| *circZfp426* | 5'- GGCCACAGTAGGGTATCAGC -3' | 5'- GTCCTCTGAAGGACCTGGGAA -3' |
| *circVps41* | 5'- GTCGTCGTAGCCAAGGAACG -3' | 5'- CAAACAGCAGCAGCAGAATCTT -3' |
| *circDdx26b* | 5'- TGGCGACAGGCTTTTGACAG -3' | 5'- GGCGTGATTTTCCTTCCAACC -3' |
| *circPak1* | 5'- AAAACCCACAGGCTGTTCTGG -3' | 5'- AGCAGCAGCAGCTACAAAGTG -3' |
| *circClec16a* | 5'- CCGCCACGAACTCAGAGAATG -3' | 5'- TGGTACAGGTACCTTTGTTATGAGA -3' |
| *circDnmt3a* | 5'- AGACTGGCCTTCTCGACTCC -3' | 5'- GATACAAATGTCTGTAGCAATCCCA -3' |
| *circPhka2* | 5'- GTTGAGCACTGCCAGAACCC-3' | 5'- GCATTCTTGCGGTAGGCCAT-3' |
| *circTjp1* | 5'- ATTCAGGTCGCTCGCATGAC-3' | 5'- ATTGCTGTGCTCTGCCATTG-3' |
| *circPhc3* | 5'- TCAGCCAACGAGACCCTTCT-3' | 5'- TGTGGTCCTTAAACCTGGTGC-3' |
| *circEgf* | 5'- TCTGTTGTTGGAGGGAGCGA-3' | 5'- TGCAAAATATATCTGGCCCTTGGA-3' |
| *circSenp1* | 5'- TAAGCCTGCCCCAAGTCCAT-3' | 5'- ACAGAATCCTCTTCTGCTGTGC-3' |
| *circCabin1* | 5'- CAGCAAGACTCACCGGAACC-3' | 5'- GTCCTGGCTTCGGTGTTGAA-3' |
| *circStrn3* | 5'- CCGCAACAGTACACGATCCC-3' | 5'- GTAAAAATGCAATCCGTGCCTG-3' |
| *circIft88* | 5'- AGCGTCTTTTGCTGTGGGTTA-3' | 5'- TGCTCTCACTGCTGTCATCG-3' |
| *circNnt* | 5'- CTCAACAGTGCAAGGAGGTGG-3' | 5'- CATTGAAGCCCTGCTTGACCA-3' |
| *circRims1* | 5'- CATCACAGCTCAGCCAGACAG-3' | 5'- CTATACTGCCGCTTCGGACC-3' |
| *circCasd1* | 5'- GGGAGCAAGCACAGCAATGA-3' | 5'- TCATACAACTGTGAGGTTGCCA-3' |
| *GAPDH* | 5'-AGGTCGGTGTGAACGGATTTG-3' | 5'-TGTAGACCATGTAGTTGAGGTCA-3' |

Table 2

MicroRNAs primers for qRT-PCR analysis.

| MicroRNAs | RT-Primer | Premiers |
|---|---|---|
| *miR-9-5p* | 5'-GTCGTATCCAGTGCGTGTCGTGG AGTCGGCAATTGCACTGGATACGA CTCATACA-3' | F:5'- GGGTCTTTGGTTATCTAGCTG-3' R: 5'-CAGTGCGTGTCGTGGAGT-3' |
| *mmu-U6* | 5'-CGCTTCACGAATTTGCGTGTCAT-3' | F:5'-CAAAGTGCTTACAGTGCAGGTAG-3' R: 5'-CTACCTGCACTGTAAGCACTTTG-3' |

# 2.7. Western blotting analysis

Briefly, RIPA buffer mixed with protease and phosphatase inhibitor mixtures was used to extract the proteins and the proteins were transferred onto PVDF membranes (Millipore, Bedford, MA) after separated by SDS-PAGE (7·5-12·5% polyacrylamide gels). Primary antibodies and appropriate horseradish peroxidase-conjugated secondary antibody (1:5000) were used to detect the corresponding proteins. The results were obtained using the Enhanced Chemiluminescence (ECL) Western blot System (Amersham Biosciences).

# 2.8. Osteogenic differentiation

Mouse Mesenchymal Stem Cells (mMSCs), isolated from bone marrow of C57BL/6 mice, were obtained from Cyagen Biosciences Inc (China). Identification of the cells according to the cell surface phenotypes and multipotency was performed by the supplier. mMSCs were cultured with alpha-Minimal Essential Media (α-MEM) (Invitrogen, Paisley, UK) supplemented with 10% FBS and 100 μg/ml penicillin/streptomycin. Osteoblastic differentiation of MSC was carried out using osteoblastic induction medium (OIM) containing standard growth medium supplemented with $10^{-8}$ M Dex, 50μg/ml ascorbic acid and 10 mM bglycerophosphate (Sigma-Aldrich, St Louis, USA).

# 2.9. Alkaline Phosphate (ALP) and alizarin red staining

After induced 7 days, cells were fixed with 4% formaldehyde for 30 seconds after washed with PBS twice. Alkaline Phosphatase kit (Sigma) was used to stained in dark. As for alizarin red staining, cells were stained with 40 mmol/L of Alizarin red solution (pH 4·2) for 10 minutes.

# 2.10. Co-culture

We co-cultured chondrocytes with osteoblasts in a transwell system with a 0·4-μm pore polyethylene terephthalate (PET) membrane as previous report.[14] The chondrocytes were transfected with or without

miR-9-5p for 2 days. Primary mMSCs were induced with osteogenic medium for 7 days. Thereafter, the osteoblasts were co-cultured with chondrocytes in α-MEM medium with exosome-depleted FBS for 2 days.

## 2.11. Cell transfection

The overexpression plasmid vector for mouse circStrn3 and mouse *KLF5* gene were created by Genechem (Shanghai, China). MiR-9-5p mimic, miR-NC, anti-microRNA oligonucleotides AMO-9-5p and AMO-NC were synthesized by Genechem (Shanghai, China). Chondrocytes were transfected with miR-9-5p, AMO-9-5p or plasmid DNA using Lipofectamine 3000 reagent (Invitrogen, Paisley, UK) according to the manufacturer's protocols.

## 2.12. Isolation and identification of chondrocytes-derived exosomes

The exosomes were separated from 200 mL of chondrocytes culture medium. The isolation and purification process were conducted as previously described.[15] Briefly, the culture supernatant was obtained by centrifugation at 300 × g and 2000 × g separately for 10 min to remove the floating cells and the dead cells. The supernatant was then centrifugated at 10,000 × g for 30 min to remove cell debris. This was followed by centrifugation at 10,000 × g for 70 min and the pellets were exosomes and contaminating proteins. The pellets were washed with PBS and subjected to centrifugation at 10,000 × g for 70 min again and the last pellets were the pure exosomes.

In order to identify the exosome, we extracted and observed the morphology of exosome, we conducted the transmission electron microscopy (TEM) test. Exosomes were fixed with 1% (w/v) glutaraldehyde in PBS. A drop of the mixture was loaded onto a carbon-coated grid, negatively stained with 3% (w/v) aqueous phosphotungstic acid for 1 min, and then observed under transmission electron microscopy (HITACHI, HT7700). The collected exosomes were resuspended with 1ml PBS and loaded into the sample pool of Nanosight LM 10 (Malvern) as instructed. After the sample measurement was completed, the particle size distribution was calculated. The fluorescent dye 3, 3'-dioctadecyloxacarbocyanine perchlorate (DIO) (Invitrogen Molecular Probes, Carlsbad, CA) was used to label exosomes and cell membrane.

## 2.13. Luciferase Reporter Assays

To reveal the interaction of circRNA-miRNA, circStrn3 sequence containing the putative (wild type, WT) or mutation (mutation type, Mut) target sites for miR-9-5p was synthesized and cloned into the psiCHECK2 reporter vector (Promega Corporation, Madison, WI, USA) downstream to the firefly luciferase. After 24 hours starvation in serum-free medium, HEK293 cells ($1\times10^5$ per well) were transfected with WT or Mut and cotransfected with 100 nM miR-9-5p mimics or miR-NC using Lipofectamine 3000 reagent. The cells were also transfected with 50 ng pRL-TK vector as an internal standard.

The 3'-UTR sequences of KLF5 predicted to interact with miR-9-5p was identified using TargetScan (http://www.targetscan.org). DNA fragments of the 3'-UTR of KLF5 containing the putative miR-9-5p binding sequence was cloned into the psiCHECK2 reporter vector (Promega Corporation, Madison, WI, USA) downstream to the firefly luciferase. Luciferase reporter genes were co-transfected with miR-9-5p mimics and miR-NC into HEK293 cells using Lipofectamine 3000. The cells were also transfected with 50 ng pRL-TK vector as an internal standard. Dual-Luciferase Reporter Assay System (Promega) and a luminometer (Lumat LB9507) were performed to measure the relative luciferase activity.

## 2.14. Statistical analysis

All the data were analyzed using GraphPad Prism software. The data were presented as mean ± SD. Two-sided Student's t test and one-way analysis were used to show the difference between groups. *$p < 0{\cdot}05$* and *$p < 0{\cdot}01$*, were considered statistically significant.

## 2.15. Role of funding source

Financial support was provided by National Natural Science Foundation of China. None of these sponsors had any role in the study design, the collection, analysis, and interpretation of data, the writing of the report, or the decision of paper submission.

# 3. Results

*3.1. CircStrn3 was decreased in knee articular cartilage from OA patients and mice.*

Ribo-minus RNA sequencing was firstly applied to screen dysregulated circRNAs in mechanically loaded chondrocytes. 20 most differentially expressed ($p < 0{\cdot}05$, fold change > 3) circRNAs (including 10 downregulated and 10 upregulated) were identified (Figure 1A, B). To confirm the results of RNA deep sequencing, we measured the expressions of these identified circRNAs using qRT-PCR. The results showed that during these differentially expressed circRNAs, circStrn3 was most frequently repressed in mechanically loaded chondrocytes (Figure 1C). Thus, circStrn3 was firstly selected for the further study. We then detected the expression of circStrn3 in OA cartilage from DMM mouse model and OA patients. HE staining and Safranin-O/Fast Green staining were applied to observe morphological structure of the articular cartilage. The results showed that articular cartilage in sham group mouse and non-OA patients possessed regular morphological structure. In contrast, OA mouse and OA patients exhibited evidently the reduction in chondrocytes and articular cartilage thickness with the irregular morphological structure (Figure 1D-F). The expression of circStrn3 was tested using FISH in knee articular cartilage from OA patients and mouse. The results showed that circStrn3 expression was significantly decreased, as evidenced by the lower immunofluorescent intensity of circStrn3 in OA cartilage from DMM mouse and OA patients (Figure 1D, E). We then isolated and cultured the chondrocytes from Sham group mouse and OA group mouse, followed by the analysis of qRT-PCR to test circStrn3 expression. The results showed that the expression of circStrn3 was decreased in chondrocytes from OA group mouse as compared with that from sham group mouse (Figure 1F). Similar results were also obtained from OA patients and non-OA patients (Figure 1G). Next, we designed a set of convergent primers by strn3 mRNA and divergent

primers for circStrn3 amplification using cDNA and genomic DNA (gDNA). CircStrn3 was amplified by divergent primers in cDNA but not in gDNA (Figure 1I). We used Sanger sequencing of the RT-PCR product amplified by divergent primers to confirm the head-to-tail splicing junction of circStrn3 (Figure 1H), indicating that the circStrn3 could be amplified by RT-PCR and expressed in chondrocytes. We also determined that CircStrn3 primarily located in cytoplasm by performing FISH experiments and nuclear and cytoplasmic separation qRT-PCR in chondrocytes (Figure 1J, K). These results indicated that circStrn3 may act through sponging miRNAs, given its location in cytoplasm.

*3.2. CircStrn3 was involved in the regulation of chondrocytes extracellular matrix production by mechanical stress.*

To observe the effect of circStrn3 on the chondrocytes extracellular matrix expression, the level of circStrn3 was firstly increased with plasmid expressing circStrn3. COL2α1, as a major component of the cartilage ECM, was decreased in circStrn3 overexpressed chondrocytes. However, MMP-13 and ADAM metallopeptidase with thrombospondin type 1 motif,5 (ADAMTS5), two critical enzymes for cartilage degrading, were significantly increased in chondrocytes overexpressed with circStrn3. We then tested the effect of circStrn3 on the regulation of chondrocytes extracellular matrix expression by mechanical stress. QRT-PCR and western blot analysis showed that decreasing expression of COL2α1 and increasing expressions of MMP-13 and ADAMTS5 were observed in mechanically loaded chondrocytes, which were significantly alleviated by overexpression of circStrn3 (Figure 2A-D). Similar results were further confirmed by immunofluorescence staining. The green fluorescence intensities of COL2α1 and MMP13 in tensile strain group were decreased and increased respectively, as compared with that in the control group. However, overexpression of circStrn3 obviously attenuated the inhibitory effect of tensile strain on COL2α1 expression and the promoting effect of tensile strain on MMP13 expression in chondrocytes (Figure 2E, F).

*3.3. MiR-9-5p was a complementary targeting miRNA of circStrn3.*

To explore the molecular mechanisms by which circStrn3 regulated chondrocytes extracellular matrix expression, we used bioinformatic tools to predict the putative targeting miRNAs of circStrn3. Some miRNAs were predicted to bind to circStrn3, including miR-9-5p, miR-6967-3p and miR-667-5p (data not shown). Complementation between circStrn3 and “seed sequence” of miR-9-5p were showed in Figure 3A. We tested these miRNAs expression by qRT-PCR in articular cartilage and chondrocytes from OA patients and non-OA patients. Among these microRNAs, the expression of miR-9-5p was increased (Figure 3B). FISH assay in chondrocytes from OA patients and non-OA patients also confirmed that miR-9-5p was abundant in OA patients (Figure 3C). In addition, the qRT-PCR results showed an increasing expression of miR-9 in mouse chondrocytes exposed to mechanical loading, which corresponded to the regulation of circStrn3 by mechanical loading in chondrocytes (Figure 3D). We transfected the mouse chondrocytes with circStrn3 overexpression plasmid and the qRT-PCR results showed that miR-9-5p was significantly decreased in circStrn3 overexpressed chondrocytes (Figure 3E, F). The sequence of circStrn3 was inserted into the 3'-UTR of the psiCHECK2 plasmid (wild type, WT) to construct dual-luciferase reporter system,

which was used to verify whether circStrn3 acted through sponging miR-9-5p directly. The results showed a significant decrease in the firefly luciferase activity when WT was cotransfected with miR-9-5p mimics (Figure 3G). We then cloned two mutated sequences into 3'-UTR of psiCHECK2 plasmid (Mutation type, Mut), which were binding sites for miR-9-5p in circStrn3 mutated. No significant change was observed in luciferase activity after co-transfection with Mut and miR-9-5p mimic (Figure 3G), suggesting that miR-9-5p may be a high-affinitive target of circStrn3 in chondrocytes. After that, we performed FISH and confirmed that circStrn3 co-localized with miR-9-5p in the cytoplasm (Figure 3H). Taken together, these results suggested that miR-9-5p may be a high-affinitive target of circStrn3 in chondrocytes.

To further examine whether miR-9-5p was involved in the regulation of chondrocytes extracellular matrix production, miR-9-5p was overexpressed or silenced in chondrocytes with miR-9-5p mimic and AMO-9-5p respectively. QRT-PCR analysis indicated that the expression of COL2α1 was increased, and the expressions of MMP-13 and ADAMTS-5 were obviously decreased in chondrocytes transfected with miR-9-5p mimics compared to negative control group and the results were completely opposite while chondrocytes were transfected with AMO-9-5p (Figure 4A-C). Similar results were obtained by western blot analysis (Figure 4D) and immunofluorescence assay (Figure 4E, F). To investigate whether circStrn3 was involved in mechanical stress-mediated chondrocytes ECM production through 'sponging' miR-9-5p, circStrn3 and miR-9-5p were overexpressed in chondrocytes exposed to mechanical loading. We found that overexpression of circStrn3 promoted the downregulation of col2α1 expression and upregulation of MMP13 and ADAMTS5 expressions by mechanical loading in chondrocytes, which could be attenuated by overexpression of miR-9-5p (Figure 4G). Taken together, these results indicated that miR-9-5p targeted by circStrn3 was involved in the regulation of chondrocytes extracellular matrix production by mechanical stress in chondrocytes.

*3.4. Exosomal with high miR-9-5p from chondrocytes inhibited osteoblast differentiation.*

To characterize the vesicles released in mechanical loaded chondrocytes, the medium was then collected and ultracentrifugated to analysis vesicles. The scanning electron microscope (SEM) imaging showed that the exosomes exhibited classical typical sphere-shaped bilayer membrane structure with the diameter of about 100 nm (Figure 5A). The size distribution of isolated exosomes was 92.84±32.68nm in chondrocytes (Figure 5B). Western blot analysis of exosome markers, including CD63, CD81 and HSP70, in the extracts confirmed the presence of exosomes (Figure 5C). To confirm whether the osteoblasts could take up exosomes derived from chondrocytes, the chondrocytes were labelled using green fluorescent lipophilic (Vybrant DiO). Osteoblasts were then cocultured with chondrocytes for 24h. Confocal imaging showed numerous Dio particles were observed within osteoblasts (Figure 5D). The level of miR-9-5p in osteoblasts cocultured with control chondrocytes was obviously lower than that cocultured with mechanical loaded chondrocytes (Figure 5E).

To confirm whether exosomes carrying miR-9-5p from chondrocytes could affect osteoblasts differentiation, we collected exosomes from chondrocytes overexpressed with miR-9-5p. We added these exosomes into MSCs cultured in osteogenic differentiation medium for 7 days, followed by the

measurement of osteoblasts marker genes (*ALP*, *Runx2* and *Osterix*) expressions using qRT-PCR and immunofluorescence. The results showed that the expressions of *ALP*, *Runx2* and *Osterix* were decreased in osteoblasts adding exosomes from chondrocytes overexpressed with miR-9-5p (Figure 5F, G). We then decreased miR-9-5p expression in chondrocytes with AMO-9-5p, followed by collection of exosomes. QRT-PCR and immunofluorescence analysis showed that the expressions of *ALP*, *Runx2* and *Osterix* were increased in osteoblasts adding exosomes from chondrocytes transfected with AMO-9-5p when compared with those from chondrocytes transfected with AMO-NC (Figure 5F, G). ALP staining and Alizarin Red Staining further demonstrated that exosomes with high miR-9-5p from chondrocytes inhibited osteoblasts differentiation, whereas inhibition of miR-9-5p attenuated this effect (Figure 5H). Taken together, these results indicated that exosomes with high miR-9-5p expression from mechanical loaded chondrocytes had protective effect on increased bone remodeling of subchondral bone in OA.

*3.5. The identification of molecular target of miR-9-5p.*

Based on the above results, miR-9-5p was confirmed to involve in ECM metabolism and osteoblasts differentiation. Thus, miR-9-5p might target several regulatory factors associated with ECM metabolism and osteoblastogenesis. To address this issue, a computation and bioinformatics-based approach was used to predict the putative targets of miR-9-5p through TargetScan. These explorations lead to the identification of candidate targets of miR-9-5p: KLF5, which were confirmed to involve in ECM metabolism and osteoblastogenesis. The the unique sites of miRNA::mRNA complementarity of miR-9-5p targeting KLF5 was showed in Figure 6A. The results of western blot showed the expression of KLF5 was increased in chondrocytes from OA mice compared to sham mouse (Figure 6B, C). MiR-9-5p obviously decreased the expression of KLF5 in chondrocytes and osteoblasts. However, the level of KLF5 expression was upregulated by AMO-9-5p in chondrocytes and osteoblasts (Figure 6D-G). To further investigate whether miR-9-5p binds to the 3'-UTR of KLF5, we performed a luciferase reporter assay. We placed the 3'-UTRs of KLF5 into the 3'-UTR of a luciferase reporter plasmid to construct chimeric vectors. Luciferase activity was diminished in the reporter containing the 3'-UTR of KLF5 treated with miR-9-5p compared with pMIR-KLF5 alone, suggesting that KLF5 was the target gene of miR-9-5p (Figure 6H).

*3.6. The therapeutic effect of microRNA-9 in DMM-induced OA mice.*

To investigate the therapeutic effect of miR-9-5p on OA *in vivo*, exosomes with high miR-9-5p expression was injected into the IA joint cavity of DMM-induced OA mice. X-ray images showed that exacerbated OA pathology was found in DMM-operated mice, whereas injection of exosomal miR-9-5p into joint cavity clearly ameliorated DMM-induced OA pathology (Figure 7A). Furthermore, μCT imaging was used to determine changes in bone architecture and bone mineral density in mice model. The reduction of chondrocytes and articular cartilage thickness with the irregular morphological structure were showed in OA mice at 12w post DMM surgery. However, injection of exosomal miR-9-5p into joint cavity could obviously attenuate DMM-induced OA mice (Figure 7B). H&E staining and safranin Ofast green staining (Figure 7C, D) were applied to evaluate the hisotopathologically of articular cartilage tissues. Surface discontinuity and denudation erosion was observed in OA group. Compared with the OA group and

OA+miR-NC group, OA+miR-9-5p group presented the improvement of the morphological integrity, less severe lesion and decreased surface denudation. According to the results of safranin Ofast green staining, the OARSI score (Figure 7E) of OA+miR-9-5p group was lower than OA group and OA+miR-NC group. In addition, depth of cartilage lesions was reduced in OA+miR-9-5p group (Figure 7F). Immunohistochemistry staining showed that the intensity of the immunostaining of col2α1 was reduced in the articular cartilage of OA mouse, which was attenuated in OA mouse injected with exosomal miR-9-5p. Oppositely, the immunostaining of MMP13 was increased in the articular cartilage of OA mouse, while injection of exosomal miR-9-5p into the IA joint cavity of OA mice obviously decreased the expression of MMP13 (Figure 7G). All these results indicated that miR-9-5p could inhibit the injure of articular cartilage and provide a potential application for the treatment of OA.

# 4. Discussion

CircRNAs involve in the regulation of articular cartilage degradation caused by inflammatory factors or oxidative stress.[16] We rigorously document here the pivotal role of circStrn3 in cartilage development and OA pathogenesis using an RNA sequencing together with large scale patient data sets and experimental mouse models of OA. Further studies showed that circStrn3 inhibited matrix metabolism of chondrocytes through competitively 'sponging' miR-9-5p targeting KLF5. Exosomes with high miR-9-5p expression from chondrocytes inhibited osteoblast differentiation. In a more therapeutically oriented approach, our results revealed that local IA administration of exosomal miR-9-5p in OA mice could maintain chondrocytes normal phenotype and even reversed cartilage degradation. Taken together, these results indicated that circStrn3/miR-9-5p/ KLF5 network, crucial factors for articular cartilage degradation and sclerosis subchondral bone, may be used as therapeutic targets for OA.

Our results demonstrated for the first time that circStrn3 was important for the development of OA. Indeed, circStrn3 has been confirmed to involve in many diseases. Li *et al.* found that circStrn3 might be a potential biomarker for bone cancer pain through regulating cancer cell apoptosis and proliferation.[17] Chen *et al.* found that the knockdown of circStrn3 effectively inhibited cell proliferation and promoted epithelial mesenchymal transition in glomerular mesangial cells.[18] Furthermore, Thum *et al.* confirmed that circStrn3 was regulated on doxorubicin treatment in the heart. Knockdown of circStrn3 increased the susceptibility of cardiac to doxorubicin in cardiotoxicity.[19] However, no studies were identified that circStrn3 was a critical factor for OA. In the present study, we found that the expression of circStrn3 was obviously decreased in chondrocytes from OA patients and OA mouse. Overexpression of circStrn3 could promote the inhibition of chondrocytes extracellular matrix production by mechanical stress. Thus, the decreasing expression of circStrn3 in OA was not a pathogenically factor for OA. On the contrary, the inhibition of circStrn3 might be a protective response of chondrocytes to abnormal mechanical stimulation in OA.

In this study, bioinformatic tools were firstly used to predict the putative targeting miRNAs of circStrn3. Some miRNAs were predicted to bind to circStrn3. Among these miRNAs, miR-9-5p was selected for further study based on its expression level. Snela *et al.* found that expression of miR-9-5p was

significantly upregulated in OA tissues (patients vs. control group), which was consistent with our results.[20] We found that miR-9-5p could increase the expression of col2α1 and decrease the expressions of MMP13 and adamts5. Furthermore, exosomes with high miR-9-5p expression inhibited osteogenic differentiation of MSCs. These results indicated that miR-9-5p was a protective factor for OA. Similar conclusions were also drawn in previous studies. Tan *et al.* found that overexpression of miR-9-5p suppressed chondrocytes apoptosis and promoted cartilage remodeling through downregulating of Tnc in mice with OA.[21] In addition, Jin *et al.* found that BM-MSC-derived exosomal miR-9-5p could influence OA progression by inhibiting syndecan-1.[22] All these studies suggested that miR-9-5p could alleviate OA, even if through different regulation pathways.

Our finding that chondrocyte-derived exosomes with high miR-9-5p expression inhibited osteoblasts differentiation was an important mechanism for miR-9-5p to alleviate OA. The effects of miR-9-5p on osteoblasts differentiation were also observed in previous studies. Jia *et al.* found that the expression of miR-9-5p was downregulated in human bone marrow mesenchymal stem cells (hBMSCs) from osteoporotic patients and confirmed that miR-9-5p inhibited the osteogenic differentiation of hBMSCs.[23] Lu *et al.* found that miR-9-5p reduced skeletal cell count and cell proliferation and impaired osteoblasts differentiation. Furthermore, they also confirmed that miR-9-5p impaired bone formation through induction of osteoblasts apoptosis.[24] Although our studies did not observe the effects of exosomal miR-9-5p on osteoblasts apoptosis or proliferation, injection of exosomal miR-9-5p into joint cavity clearly ameliorated DMM-induced subchondral bone remodeling, suggested that miR-9-5p might be a hypothetical candidate for the treatment of OA and inspired a new approach to develop potential therapeutic agents treating degenerative joints as a whole organ.

Exosomes play an important role in cell-cell communication, which do not need cell contact, as that can result in a relatively long-distance influence. Exosome contains RNA components including mRNA and microRNA, which are protected by exosomes rigid membranes. Growing studies suggested that exosomes carrying miRNAs were involved in the pathogenesis of OA.[25] Most of these studies focused on the role of exosomes derived from stem cells or synovial fibroblasts in the treatment of OA.[26,27] Zhang *et al.* found exosomes derived from miR-140-5p-overexpressed human synovial MSCs enhanced cartilage tissue regeneration and prevented OA of the knee in a rat model.[28] Yuan *et al.* found that the fibroblast-like synoviocyte derived exosomal long non-coding RNA H19 alleviated OA progression through the miR-106b-5p/TIMP2 axis.[29] However, few studies were accomplished to investigate the role of exosomes from chondrocytes on the pathogenesis of OA. Our study reported for the first time that chondrocyte-derived exosomal miR-9-5p could alleviate subchondral bone remodeling through inhibiting osteoblasts differentiation in OA.

KLF5 is a transcriptional activator that binds the promoter of target genes or acts downstream of multiple signaling pathways. Previous studies showed that KLF5 was expressed in chondrocytes and osteoblasts but not in osteoclasts.[30] Cartilage matrix degradation was impaired in $KLF5^{+/-}$ mice,[30] indicating that KLF was a critical factor for the maintenance of the metabolism of the ECM matrix. In addition, KLF5 was

also confirmed to regulate Wnt/β-catenin signaling pathway, which was very important signaling pathway for bone formation.[31] In the present study, we found that KLF5 was functional target gene for miR-9-5p-mediated the matrix metabolism of chondrocytes and osteoblasts differentiation. Taken together, these results indicated that KLF5 might be effective and feasible therapeutic target for OA.

# 5. Conclusions

In conclusion, our data provided new evidence that circStrn3-targeting miR-9-5p/ KLF5 was involved in the regulation of cartilage matrix metabolism and subchondral bone remodeling in OA. This study provided a novel understanding of the molecular mechanisms underlying OA, and inspired a new approach to develop potential therapeutic agents treating degenerative joints as a whole organ.

# 6. List Of Abbreviations

| Full names | Abbreviations | Full names | Abbreviations |
|---|---|---|---|
| Osteoarthritis | OA | Collagen type II α 1 | Col2α1 |
| kruppel-like factor 5 | KLF5 | matrix metalloproteinase 13 | MMP13 |
| Circular RNAs | circRNAs | fetal bovine serum | FBS |
| microRNAs | miRNAs | fluorescence in situ hybridization | FISH |
| 3'-untranslational region | 3'-UTR | complementary DNA | cDNA |
| intra-articular | IA | Mouse Mesenchymal Stem Cells | mMSCs |
| destabilized medial meniscus | DMM | alpha-Minimal Essential Media | α-MEM |
| Enhanced Chemiluminescence | ECL | osteoblastic induction medium | OIM |
| polyethylene terephthalate | PET | transmission electron microscopy | TEM |
| dioctadecyloxacarbocyanine | DIO | wild type | WT |
| mutation type | Mut | genomic DNA | gDNA |
| scanning electron microscope | SEM | human bone marrow mesenchymal stem cells | hBMSCs |

# 7. Declarations

***Ethics approval and consent to participate***

Not applicable.

### *Consent for publication*

Not applicable.

### *Availability of data and materials*

All data generated or analysed during this study are included in this published article and its supplementary information files.

### *Competing interests*

The authors declare that they have no competing interests.


### *Funding*

This work was supported by National Science Foundation of China, Shanghai Talent Development Funding Scheme and the Science and Technology Commission of Shanghai Municipality.


### *Authors' contributions*

LG, BL and FQH conceived the study; TD and HYC collected the data; CEL, BC XX and PH analyzed and interpreted the data; BL, FQH, TD and HYC performed the experiments; GL, BL and TD wrote the manuscript. All authors reviewed and approved the final manuscript.


### *Acknowledgements*

Not applicable.


# 8. References


1. Fan G, Liu J, Zhang Y, Guan X. LINC00473 exacerbates osteoarthritis development by promoting chondrocyte apoptosis and proinflammatory cytokine production through the miR-424-5p/LY6E axis. *Exp Ther Med* 2021; 22(5):1247.
2. Egloff C, Hart DA, Hewitt C, Vavken P, Valderrabano V, Herzog W. Joint instability leads to long-term alterations to knee synovium and osteoarthritis in a rabbit model. *Osteoarthritis Cartilage* 2016; 24(6):1054-1060.
3. Zhong D, Chen XI, Zhang W, Luo ZP. Excessive tensile strain induced the change in chondrocyte phenotype. *Acta Bioeng Biomech* 2018; 20(2):3-10.
4. Lu J, Zhang H, Cai D, et al. Positive-Feedback Regulation of Subchondral H-Type Vessel Formation by Chondrocyte Promotes Osteoarthritis Development in Mice. *J Bone Miner Res* 2018; 33(5):909-920.
5. Yu H, Wang X, Cao H. Construction and investigation of a circRNA-associated ceRNA regulatory network in Tetralogy of Fallot. *BMC Cardiovasc Disord* 2021; 21(1):437.

6. Jiao P, Wang XP, Luoreng ZM, et al. MiR-223: An Effective Regulator of Immune Cell Differentiation and Inflammation. *Int J Biol Sci* 2021; 17(9):2308-2322.
7. Malka Y, Steiman-Shimony A, Rosenthal E, et al. Post-transcriptional 3 -UTR cleavage of mRNA transcripts generates thousands of stable uncapped autonomous RNA fragments. *Nat Commun* 2017; 8(1):2029.
8. Zhang D, Lee H, Zhu Z, Minhas JK, Jin Y. Enrichment of selective miRNAs in exosomes and delivery of exosomal miRNAs in vitro and in vivo. *Am J Physiol Lung Cell Mol Physiol* 2017; 312(1):L110-L121.
9. Shan SK, Lin X, Li F, et al. Exosomes and Bone Disease. *Curr Pharm Des* 2019; 25(42):4536-4549.
10. Li J, Zhang B, Liu WX, et al. Metformin limits osteoarthritis development and progression through activation of AMPK signalling. *Ann Rheum Dis* 2020; 79(5):635-645.
11. Chen K, Yan Y, Li C, et al. Increased 15-lipoxygenase-1 expression in chondrocytes contributes to the pathogenesis of osteoarthritis. *Cell Death Dis* 2017; 8(10):e3109.
12. Song T, Ma J, Guo L, Yang P, Zhou X, Ye T. Regulation of Chondrocyte Functions by Transient Receptor Potential Cation Channel V6 in Osteoarthritis. *Journal of cellular physiology* 2017.
13. Shen P, Yang Y, Liu G, et al. CircCDK14 protects against Osteoarthritis by sponging miR-125a-5p and promoting the expression of Smad2. *Theranostics* 2020; 10(20):9113-9131.
14. Sun W, Zhao C, Li Y, et al. Osteoclast-derived microRNA-containing exosomes selectively inhibit osteoblast activity. *Cell discovery* 2016; 2:16015.
15. Van De Vlekkert D, Qiu X, Annunziata I, d'Azzo A. Isolation, Purification and Characterization of Exosomes fromFibroblast Cultures of Skeletal Muscle. *Bio Protoc* 2020; 10(7):e3576.
16. Shen S, Wu Y, Chen J, et al. CircSERPINE2 protects against osteoarthritis by targeting miR-1271 and ETS-related gene. *Ann Rheum Dis* 2019; 78(6):826-836.
17. Zhang Y, Zhang X, Xing Z, et al. CircStrn3 is involved in bone cancer pain regulation in a rat model. *Acta Biochim Biophys Sin (Shanghai)* 2020; 52(5):495-505.
18. Ling L, Tan Z, Zhang C, et al. CircRNAs in exosomes from high glucose-treated glomerular endothelial cells activate mesangial cells. *Am J Transl Res* 2019; 11(8):4667-4682.
19. Gupta SK, Garg A, Bar C, et al. Quaking Inhibits Doxorubicin-Mediated Cardiotoxicity Through Regulation of Cardiac Circular RNA Expression. *Circ Res* 2018; 122(2):246-254.
20. Kopanska M, Szala D, Czech J, et al. MiRNA expression in the cartilage of patients with osteoarthritis. *J Orthop Surg Res* 2017; 12(1):51.
21. Chen H, Yang J, Tan Z. Upregulation of microRNA-9-5p inhibits apoptosis of chondrocytes through downregulating Tnc in mice with osteoarthritis following tibial plateau fracture. *J Cell Physiol* 2019; 234(12):23326-23336.
22. Jin Z, Ren J, Qi S. Exosomal miR-9-5p secreted by bone marrow-derived mesenchymal stem cells alleviates osteoarthritis by inhibiting syndecan-1. *Cell Tissue Res* 2020; 381(1):99-114.

23. Zheng C, Bai C, Sun Q, et al. Long noncoding RNA XIST regulates osteogenic differentiation of human bone marrow mesenchymal stem cells by targeting miR-9-5p. *Mech Dev* 2020; 162:103612.
24. Sun T, Leung F, Lu WW. MiR-9-5p, miR-675-5p and miR-138-5p Damages the Strontium and LRP5-Mediated Skeletal Cell Proliferation, Differentiation, and Adhesion. *Int J Mol Sci* 2016; 17(2):236.
25. Asghar S, Litherland GJ, Lockhart JC, Goodyear CS, Crilly A. Exosomes in intercellular communication and implications for osteoarthritis. *Rheumatology (Oxford)* 2020; 59(1):57-68.
26. Mianehsaz E, Mirzaei HR, Mahjoubin-Tehran M, et al. Mesenchymal stem cell-derived exosomes: a new therapeutic approach to osteoarthritis? *Stem Cell Res Ther* 2019; 10(1):340.
27. Liu Y, Lin L, Zou R, Wen C, Wang Z, Lin F. MSC-derived exosomes promote proliferation and inhibit apoptosis of chondrocytes via lncRNA-KLF3-AS1/miR-206/GIT1 axis in osteoarthritis. *Cell Cycle* 2018; 17(21-22):2411-2422.
28. Tao SC, Yuan T, Zhang YL, Yin WJ, Guo SC, Zhang CQ. Exosomes derived from miR-140-5p-overexpressing human synovial mesenchymal stem cells enhance cartilage tissue regeneration and prevent osteoarthritis of the knee in a rat model. *Theranostics* 2017; 7(1):180-195.
29. Tan F, Wang D, Yuan Z. The Fibroblast-Like Synoviocyte Derived Exosomal Long Non-coding RNA H19 Alleviates Osteoarthritis Progression Through the miR-106b-5p/TIMP2 Axis. *Inflammation* 2020; 43(4):1498-1509.
30. Shinoda Y, Ogata N, Higashikawa A, et al. Kruppel-like factor 5 causes cartilage degradation through transactivation of matrix metalloproteinase 9. *J Biol Chem* 2008; 283(36):24682-24689.
31. Zhang X, Lou Y, Zheng X, et al. Wnt blockers inhibit the proliferation of lung cancer stem cells. Drug Des *Devel Ther* 2015; 9:2399-2407.

# Figures

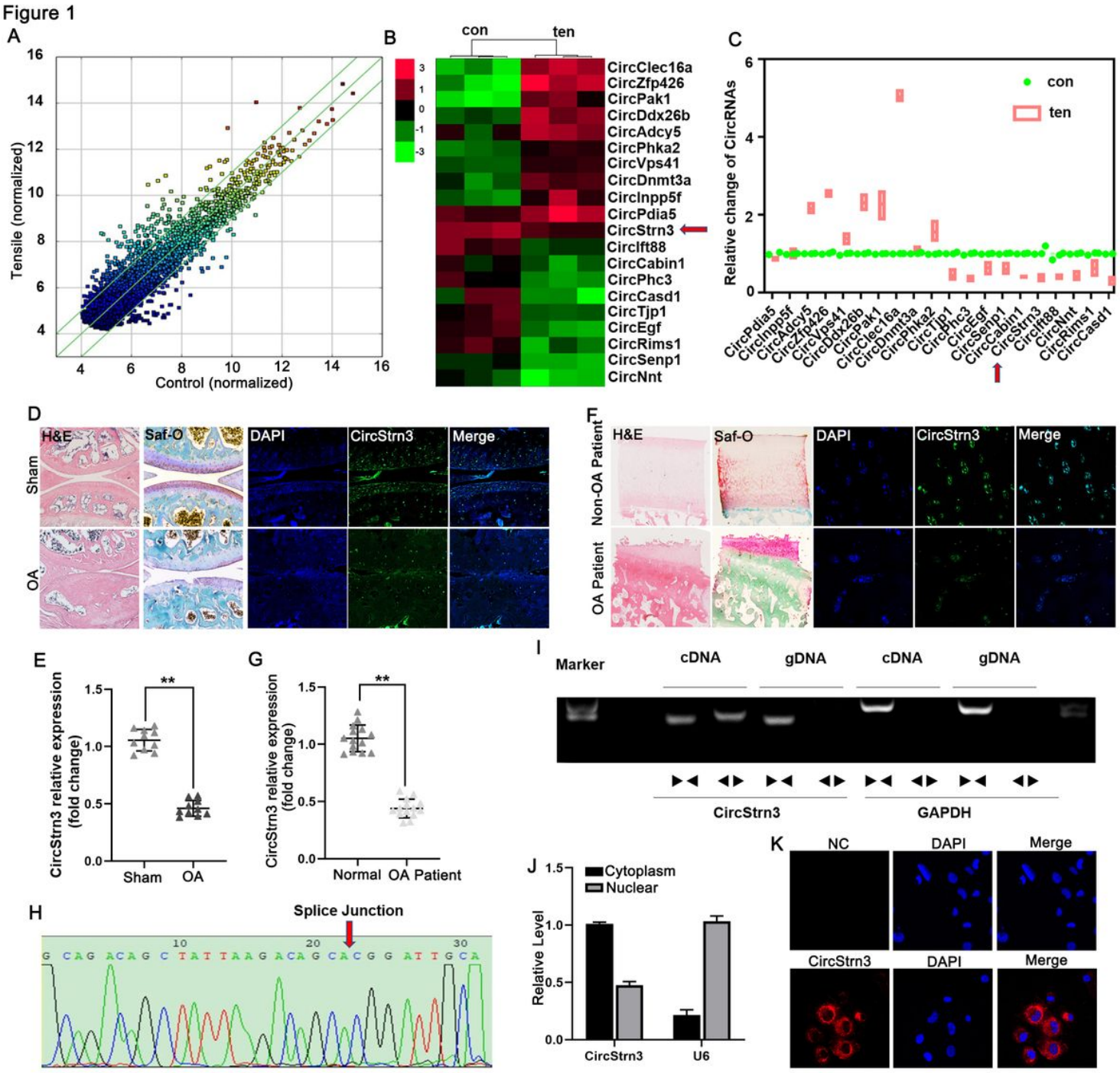


## Figure 1

CircStrn3 was decreased in knee articular cartilage from OA patients and mice. (A) Differentially expressed circRNAs found by ribo-minus RNA sequencing. n = 3. (B) Heat map representation of circRNAs differentially expressed in mechanically loaded chondrocytes. Red indicates circRNAs induced, and green indicates circRNAs repressed. n = 3. (C) RNA sequencing results were validated by qRT-PCR in mechanically loaded chondrocytes. (D) HE staining and Safranin-O/Fast Green staining were applied to observe morphological structure of the articular cartilage in OA mice. FISH staining results showed that circStrn3 was downregulated in OA mice cartilage. n = 4. (E) The results of qRT-PCR showed that the expression of circStrn3 was decreased in chondrocytes from OA mice. n = 4, **P < 0·01. (F) HE staining

and Safranin-O/Fast Green staining were applied to observe morphological structure of the articular cartilage in OA patients. FISH staining results showed that circStrn3 was downregulated in OA patients. n = 6. (G) The results of qRT-PCR showed that the expression of circStrn3 was decreased in chondrocytes from OA patients. n = 6, **P < 0·01. (H) Divergent primers detected circular RNAs in complementary DNA (cDNA), but not in genomic DNA (gDNA). (I) Sanger sequencing showed the back-splice junction (arrow) of circStrn3. (J) CircStrn3 expression was measured in nuclear and cytoplasmic separation by qRT-PCR in chondrocytes. n = 4, **P < 0·01. (k) FISH staining results showed that circStrn3 was downregulated in mechanically loaded chondrocytes. n = 4.

Figure 2

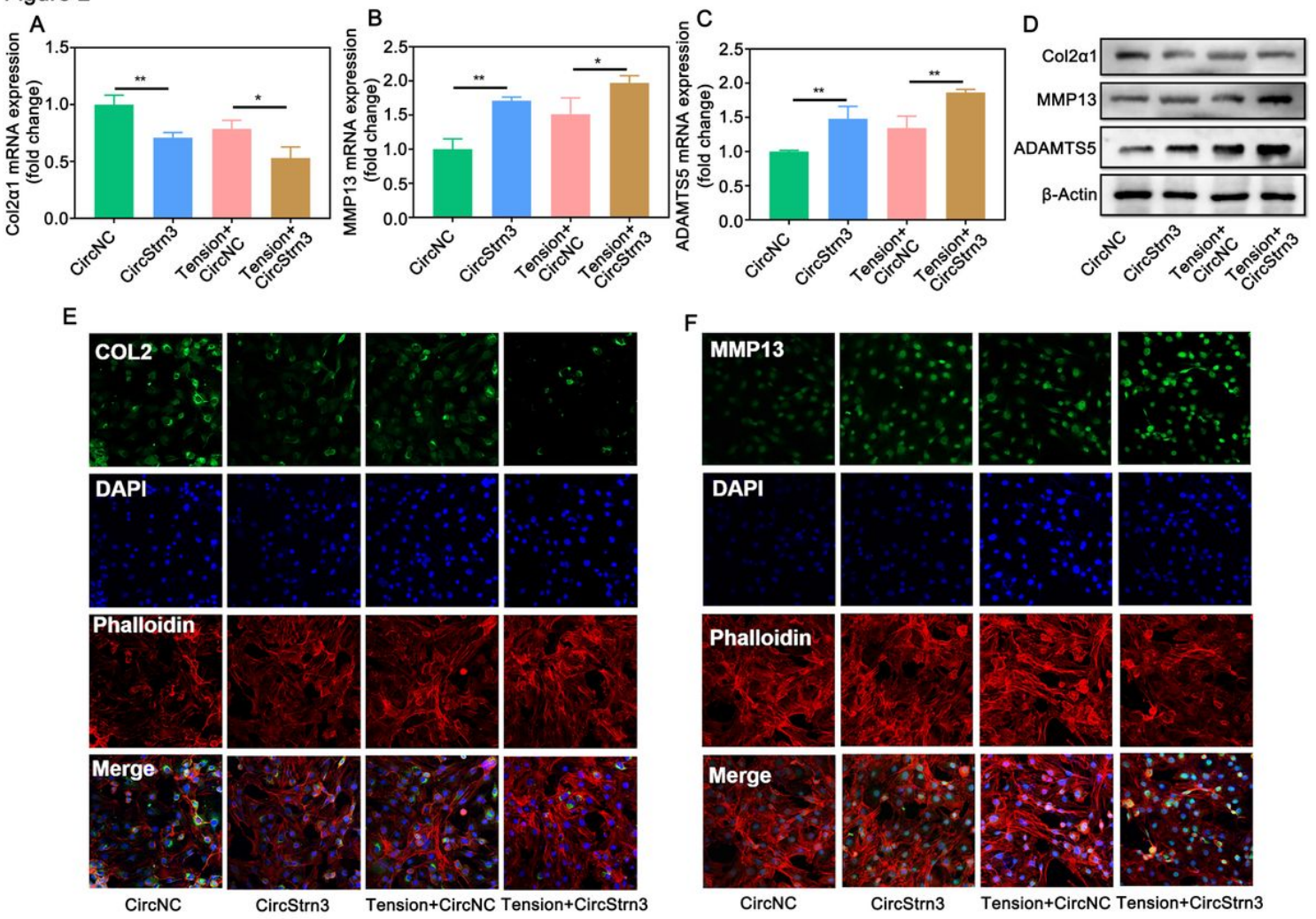


## Figure 2

CircStrn3 was involved in the regulation of chondrocytes extracellular matrix production by mechanical stress. (A-C) QRT-PCR tested the mRNA expressions of COL2α1, MMP13 and Adamts5 in chondrocytes transfected with circStrn3 or circNC, followed by stimulation of tensile strain or control condition. n = 4, *P < 0·05, **P < 0·01. (D) Western blot tested the expressions of COL2α1, MMP13 and Adamts5 in chondrocytes transfected with circStrn3 or circNC, followed by stimulation of tensile strain or control condition. n = 4. (E-F) Immunofluorescence assay tested the expressions of COL2α1 and MMP13 in

chondrocytes transfected with circStrn3 or circNC, followed by stimulation of tensile strain or control condition. n = 4.

## Figure 3

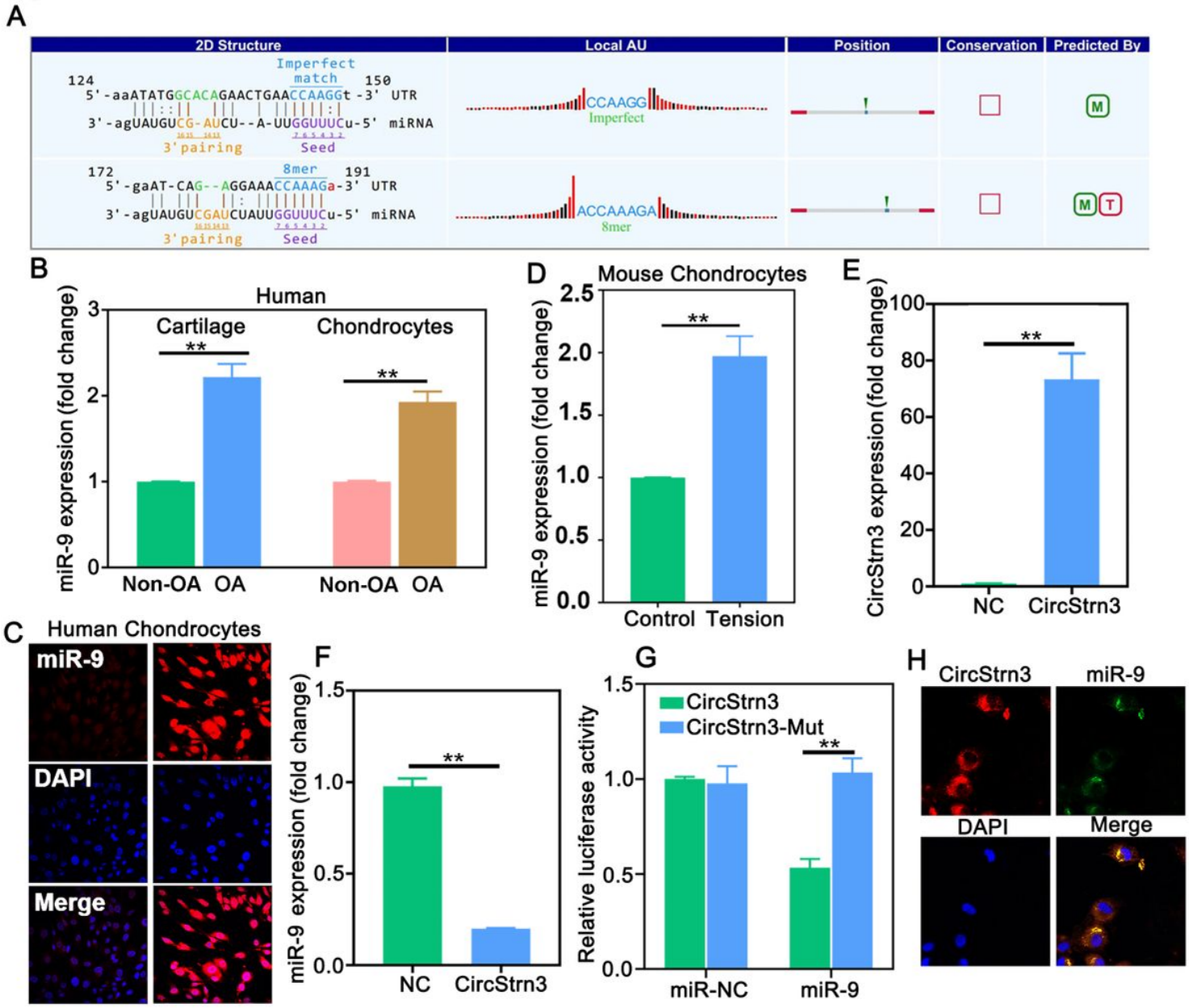


## Figure 3

CircStrn3 was involved in the regulation of chondrocytes extracellular matrix production by mechanical stress. (A) Complementation between circStrn3 and “seed sequence” of miR-9-5p. (B) The results of qRT-PCR showed that the expression of miR-9-5p was increased in cartilage and chondrocytes from OA patients. n = 4, **P < 0·01. (C) FISH staining results showed that miR-9-5p was upregulated in human chondrocytes. n = 4. (D) QRT-PCR tested the expression of miR-9-5p in chondrocytes exposed to mechanical loading or control condition. n = 4, **P < 0.001. (E-F) QRT-PCR tested the expressions of circStrn3 (e) and miR-9-5p (f) in chondrocytes transfected with circStrn3 or circNC. n = 4, **P < 0·01. (G) The results showed a significant decrease in the firefly luciferase activity when WT was cotransfected

with miR-9-5p mimics, thus no significant change was observed in luciferase activity after co-transfection with Mut and miR-9-5p mimic. n = 4, **P < 0·01. (H) FISH staining results showed that circStrn3 co-localized with miR-9-5p in the cytoplasm. n = 6.

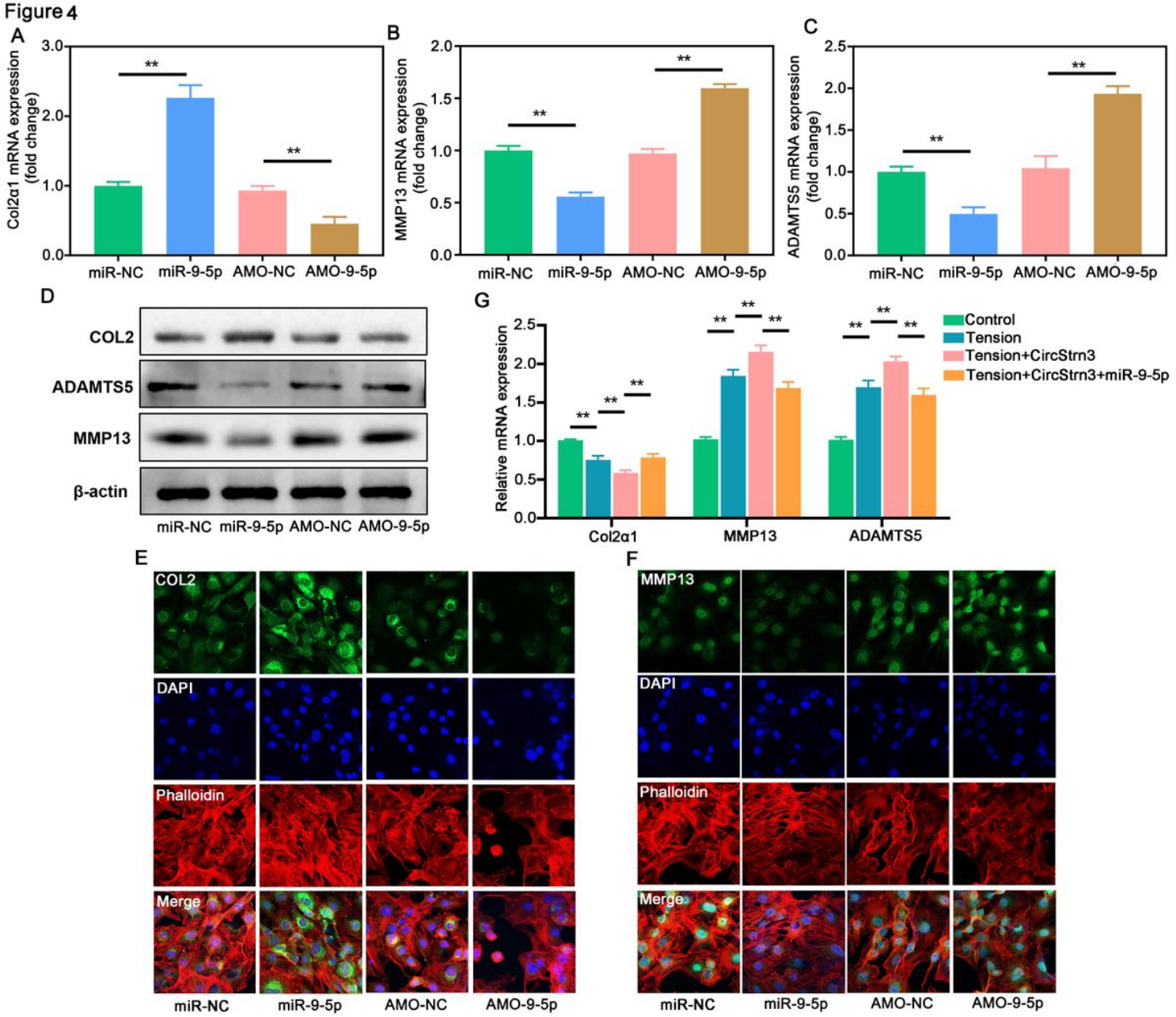


## Figure 4

MiR-9-5p was involved in the regulation of chondrocytes extracellular matrix production. (A-C) QRT-PCR tested the mRNA expressions of COL2α1, MMP13 and Adamts5 in chondrocytes transfected with miR-9-5p mimic and AMO-9-5p. n = 4, **P < 0·01. (D) Western blot tested the expressions of COL2α1, MMP13 and Adamts5 in chondrocytes transfected with miR-9-5p mimic and AMO-9-5p. n = 4. (E-F) Immunofluorescence assay tested the expressions of COL2α1 and MMP13 in chondrocytes transfected with miR-9-5p mimic and AMO-9-5p. n = 4. (G) QRT-PCR tested the mRNA expressions of COL2α1, MMP13

and Adamts5 in chondrocytes transfected with miR-9-5p mimics or circStrn3, followed by stimulation of tensile strain or control condition. n = 4, **P < 0·01.

Figure 5

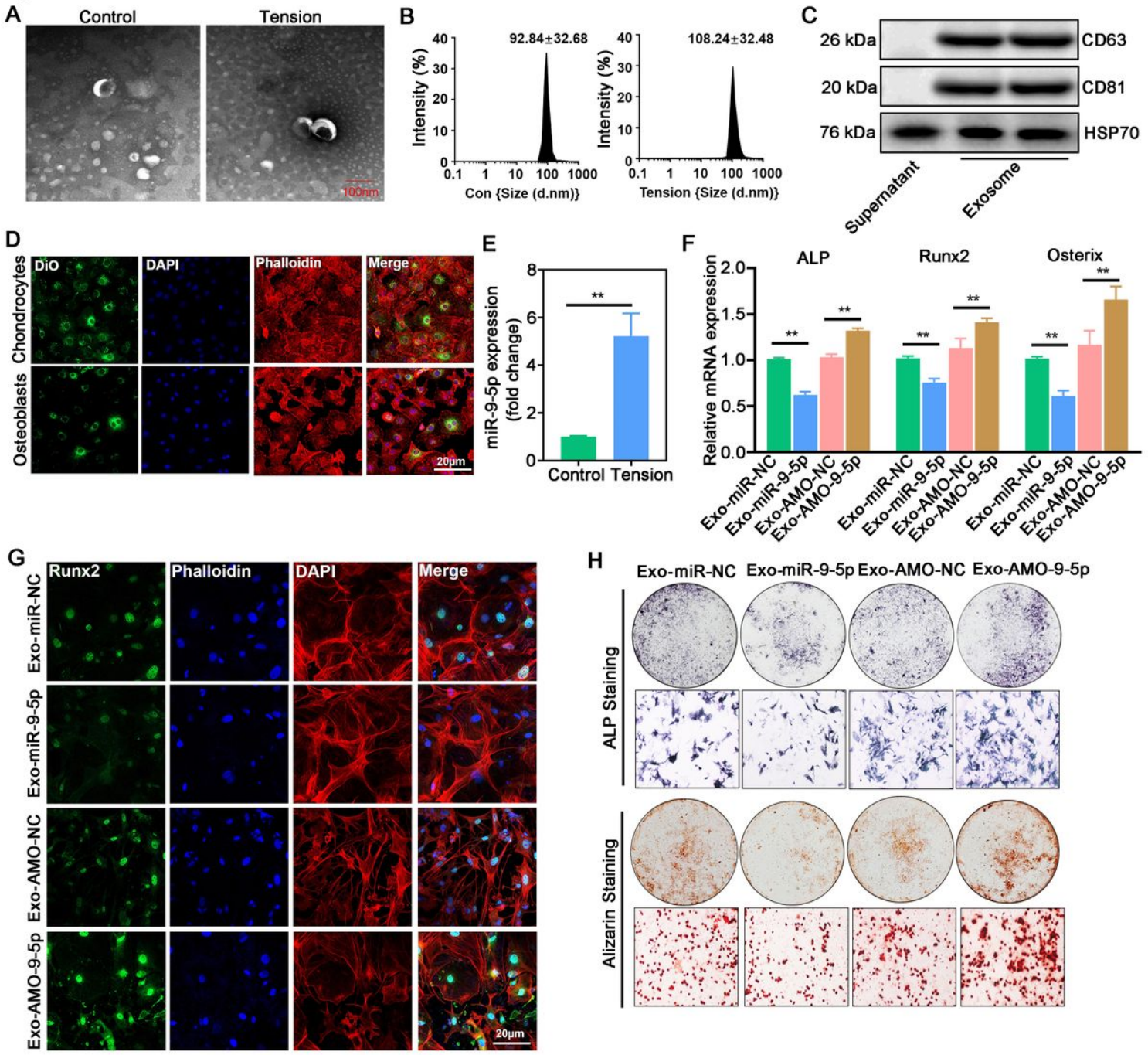


## Figure 5

Exosomal miR-9-5p from mechanical loaded chondrocytes inhibited osteoblast differentiation. (A) The SEM imaging showed that the exosomes exhibited classical typical sphere-shaped bilayer membrane structure. n = 6. Scale bars are 100 nm. (B) The SEM imaging showed that the size distribution of isolated exosomes was 92.84±32.68nm in chondrocytes. n = 6. (C) Western blot tested the expressions of CD63, CD81 and HSP70 in exosomes. n = 4. (D) Confocal imaging showed numerous Dio particles were observed within osteoblasts. Green: Chondrocytes labelled by vybrant DiO. Blue: DAPI labeling of cell

nuclei. Red: Cytoskeleton labelled by phalloidn. n = 4, Scale bars are 20 μm. (E) The results of qRT-PCR showed that the expression of miR-9-5p was increased in chondrocytes stimulated with tensile strain. n = 4, **P < 0·01. (F) QRT-PCR tested the mRNA expressions of ALP, Runx2 and Osterix in osteoblasts adding exosomes from chondrocytes transfected with miR-9-5p or AMO-9-5p. n = 4, **P < 0·01. (G) Immunofluorescence assay tested the expressions of Runx2 in osteoblasts adding exosomes from chondrocytes transfected with miR-9-5p or AMO-9-5p. n = 4. Scale bar: 20 μm. (H) Osteoblasts adding exosomes from chondrocytes transfected with miR-9-5p or AMO-9-5p. ALP and ARS staining were performed after 7 and 14 days of induction, respectively. n = 4.

**Figure 6**

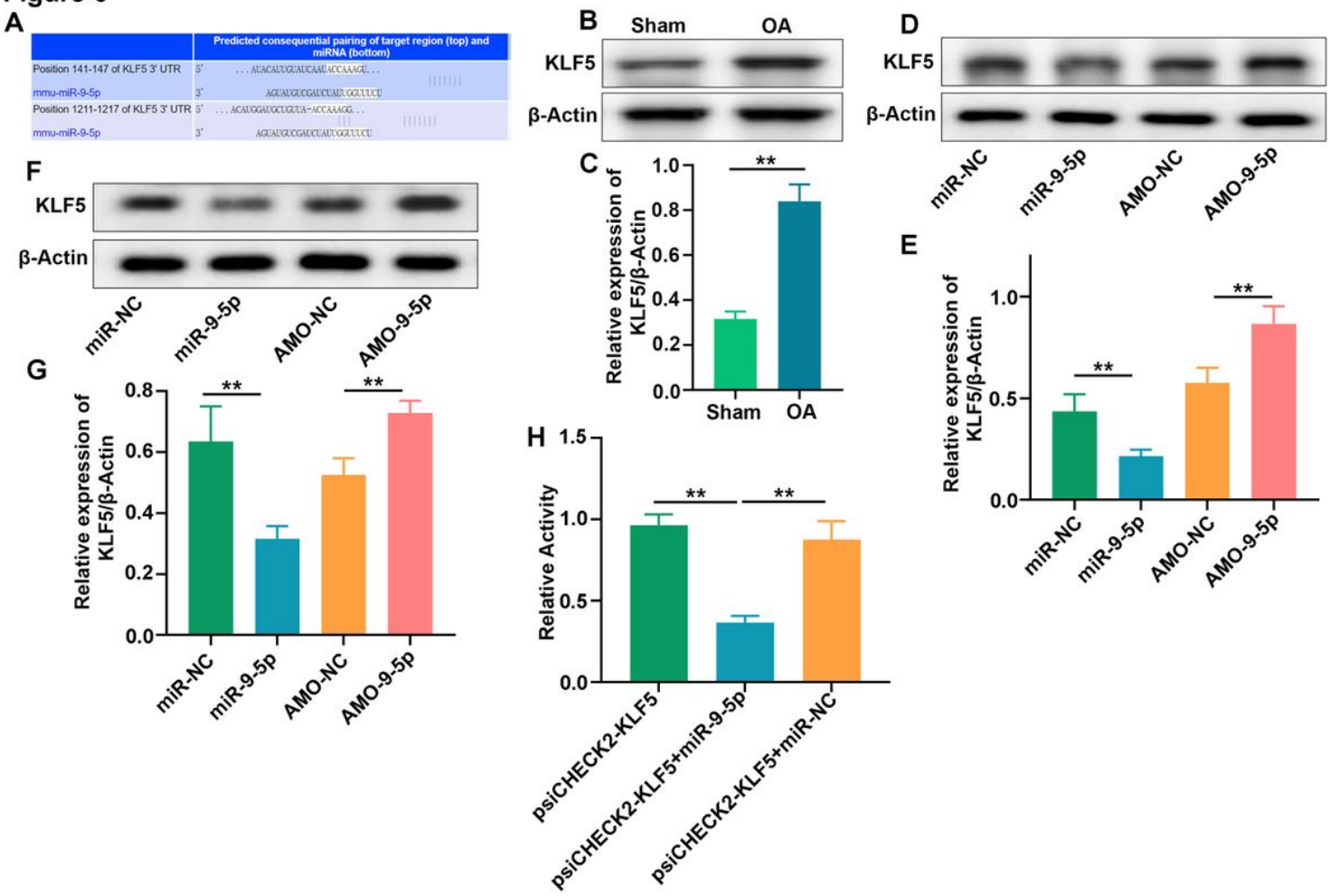


**Figure 6**

The identification of molecular target of miR-9-5p. (A) MicroRNA complementarity of miR-9-5p targeting KLF5. (B-C) The result of western blot showed the expression of KLF5 was increased in chondrocytes from OA mice compared to sham mouse. n = 4, **P < 0·01. (D-G) The results of western blot showed the level of KLF5 expression in chondrocytes(D-E) and osteoblasts(F-G) transfected with miR-9-5p or AMO-9-5p. n = 4, **P < 0·01. (H) Luciferase activity was diminished in the reporter containing the 3'-UTR of KLF5 treated with miR-9-5p compared with pMIR-KLF5 alone. n = 4, **P < 0·01.

Figure 7

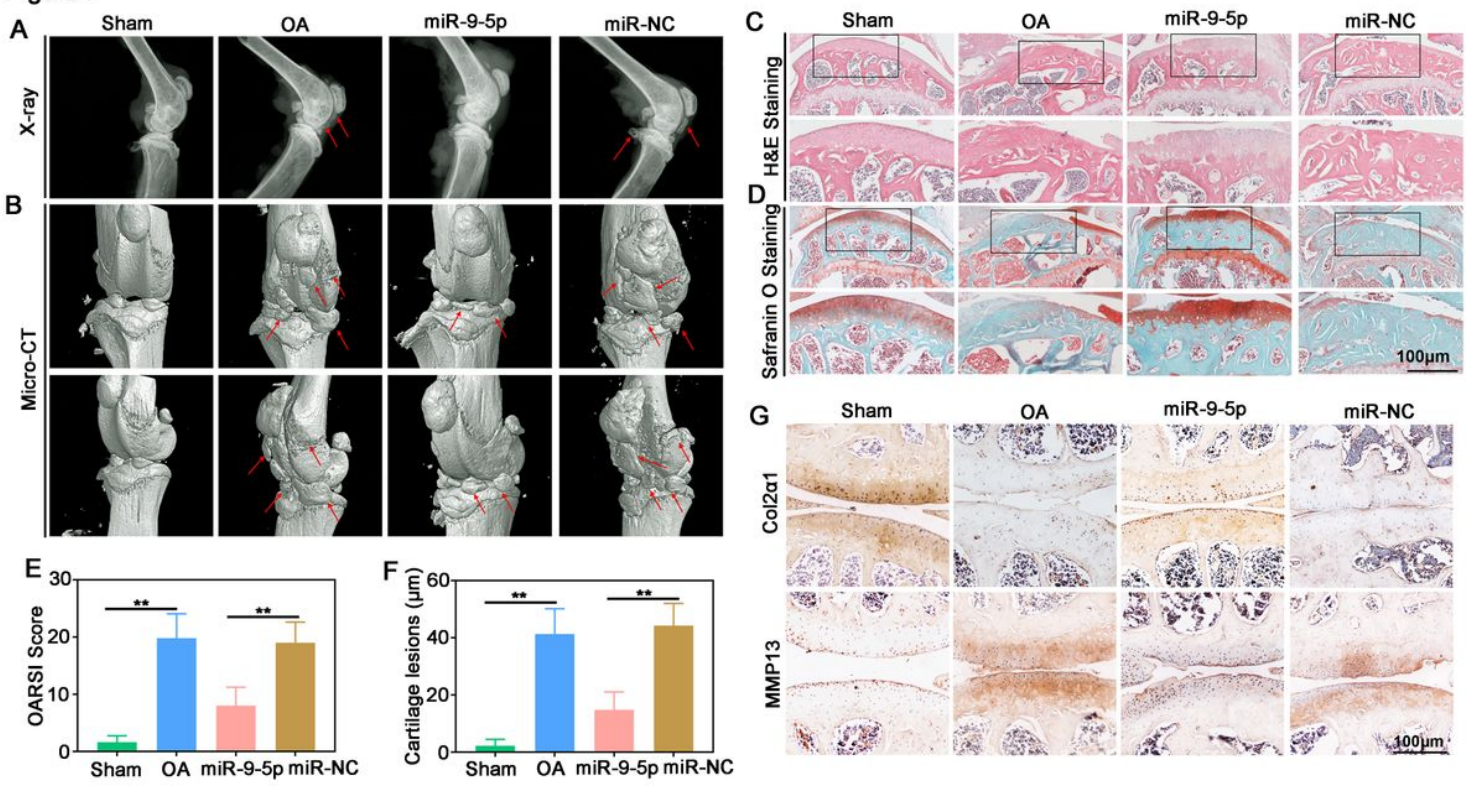


## Figure 7

The therapeutic effect of miR-9-5p in DMM-induced OA mice. (A-B) X-ray (A) and micro-CT (B) imaging for morphological structure in knee of OA rat at 12w post DMM surgery, followed by treated with IA injection of exosomes with high miR-9-5p expression and miRNA-NC, respectively. n=4. (C-D) H&E staining and safranin Ofast green staining of articular cartilage tissues of OA rat at 12w post DMM surgery, followed by treated with IA injection of exosomes with high miR-9-5p expression and miRNA-NC, respectively. n=4. Scale bar: 100 μm. (E-F) The results of safranin Ofast green staining of the OARSI score (E) and depth of cartilage lesions (F). n=4. (G) Immunohistochemistry staining showed that the intensity of the immunostaining of col2α1 and MMP13 of OA rat at 12w post DMM surgery, followed by treated with IA injection of exosomes with high miR-9-5p expression and miRNA-NC, respectively. n=4. Scale bar: 100 μm.

# Supplementary Files

This is a list of supplementary files associated with this preprint. Click to download.

- renamed5a713.docx